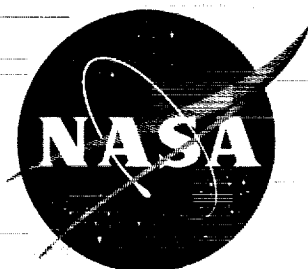IN-18
380473

TECHNICAL MEMORANDUM
X-314

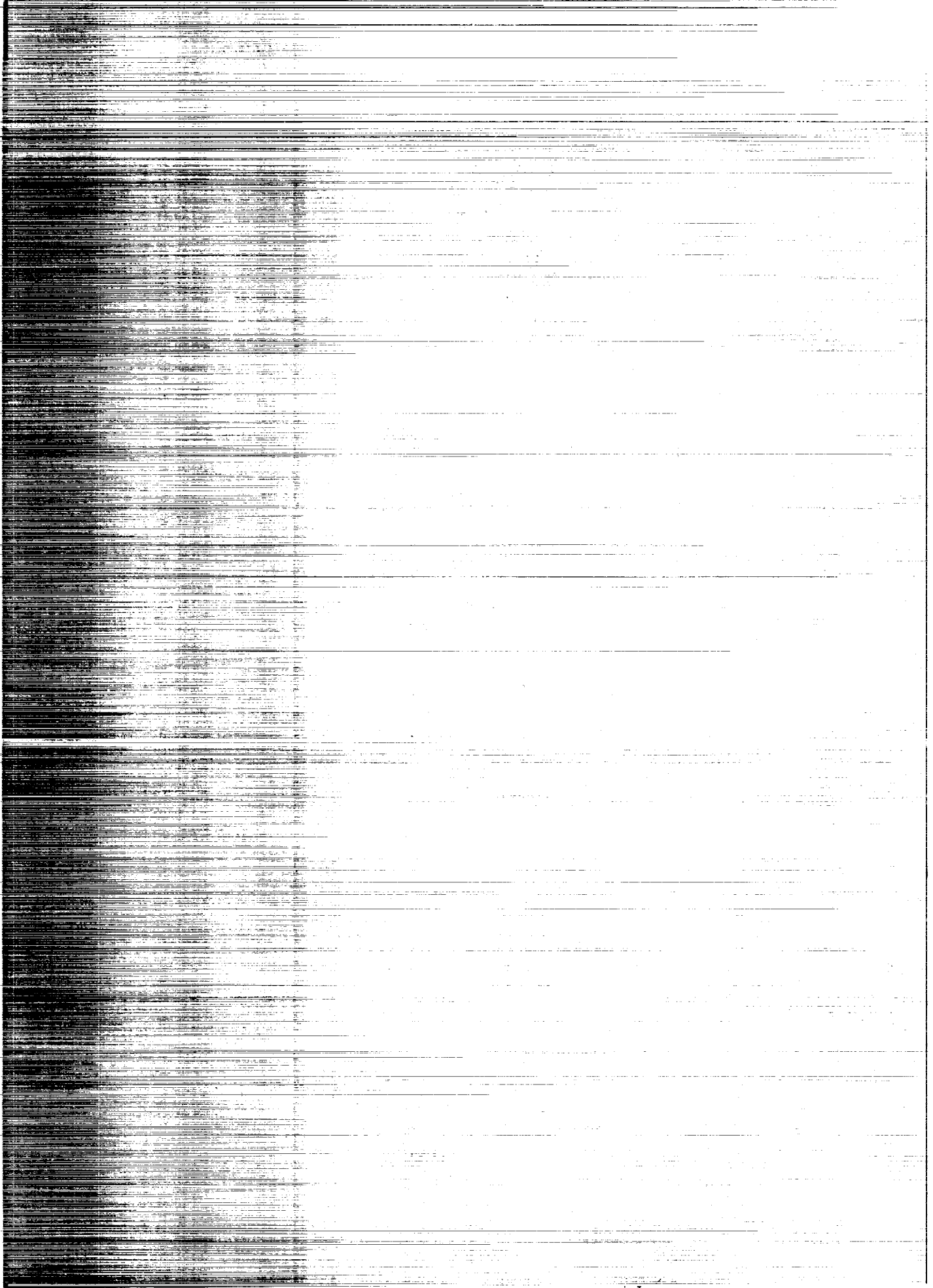EXPERIMENTAL STUDY OF A HOT STRUCTURE

FOR A REENTRY VEHICLE

By Richard A. Pride, Dick M. Royster,
and Bobbie F. Helms

Langley Research Center
Langley Field, Va.

NATIONAL AERONAUTICS AND SPACE ADMINISTRATION

WASHINGTON

September 1960
Declassified September 28, 1961

NATIONAL AERONAUTICS AND SPACE ADMINISTRATION

TECHNICAL MEMORANDUM X-314

EXPERIMENTAL STUDY OF A HOT STRUCTURE.

FOR A REENTRY VEHICLE

By Richard A. Pride, Dick M. Royster,
and Bobbie F. Helms

SUMMARY

A large structural model of a reentry vehicle has been built incorporating design concepts applicable to a radiation-cooled vehicle. Thermal-stress alleviating features of the model are discussed. Environmental tests on the model include approximately 100 cycles of loading at room temperature and 33 cycles of combined loading and heating up to temperatures of 1,600° F. Measured temperatures are shown for typical parts of the model. Comparisons are made between experimental and calculated deflections and strains. The structure successfully survived the heating and loading environments.

INTRODUCTION

Reference 1 indicates that the construction of reentry vehicles of low wing loading could be based on radiative-type structure. The load-carrying material of such vehicles would be subjected to high temperatures with large variations in temperature throughout the structure. These conditions present difficult thermal-stress problems in conventional stressed skin design (ref. 2) and have prompted investigation of structural concepts which are more suited to the thermal environment.

This paper describes the available results of a test program on a large sheet metal structure designed to cope with the heating and air loads encountered by a reentry vehicle.

STRUCTURAL DESIGN

The sheet metal structure used in the present investigation is shown in figures 1 and 2. It is triangular in planform and cross section with a length of 12 feet, a width at the back of 7 feet, and a height at the back of $2\frac{3}{4}$ feet. These dimensions provide a planform area of 47 square feet with a sweep angle of 75°. In order to provide the greatest amount of test information, this structural model was designed with one side flat and the other V-shaped. Skin panels and internal structure were symmetrically designed so that the model could be heated and loaded from either side. All parts of the structural model were fabricated from the superalloy, Inconel X.

The exterior of the model is covered with corrugated skin panels with the axis of the corrugations parallel to the flight direction. These skin panels serve a dual purpose; they carry the air loads fore and aft to the supporting internal frames, and they provide torsional stiffness for the model. Expansion joints which extend around the model cross section at 2-foot intervals help to alleviate thermal stresses but prevent the skins from contributing any bending stiffness to the model.

The internal structure is shown in figure 3. It consists of an approximately orthogonal arrangement of transverse frames and longitudinal beams. The skin-panel loads are transmitted to the transverse frames. These frames in turn transmit the loads to the two longitudinal beams. The load-carrying members operate at high temperatures because the heated skin panels radiate heat throughout the internal structure.

Corrugated shear webs are used in both transverse frames and longitudinal beams to carry the shear loads and at the same time to permit differential thermal expansion between top and bottom spar caps without a large buildup of thermal stress. Well-designed corrugated shear webs have efficient load-carrying strength and stiffness values (ref. 3). The average weight of the internal structure in this model is 1.5 lb/sq ft of wetted area, and the average weight of the skin panels is 1.0 lb/sq ft.

A closeup view of the circled region in figure 3 is shown in figure 4. This figure gives a view of an intersection of a transverse frame, longitudinal beam, and skin panels. The longitudinal shear web is a standard 60° corrugation. The spar cap consists of two channels with a cover plate and is spotwelded to the corrugated web on both sides.

The transverse shear web is a specially designed corrugation to provide extreme flexibility normal to the web between the two channels which make up the transverse cap. This flexibility is needed to allow the skin panels to expand or contract freely without large buildup of thermal stress. The transverse shear webs are spliced to the longitudinal webs at their intersection.

The skin panels are attached to the outside flanges of the transverse caps. Skin panels are fabricated by seam welding together two pieces of 0.010-inch-thick sheet. The outer sheet is beaded lightly to stiffen it against local buckling and to preset a pattern which deforms uniformly when thermal expansion across the corrugations is restrained by the underlying transverse channels. The inner sheet is formed to a $60°$, 1/2-inch flat corrugation and stops short of the edge of the outer sheet. A Z-stiffener provides the transition from the inner sheet to the outer sheet along the attached edges as shown in figure 5. The skin panels are attached only to the transverse frames and do not come in contact with the longitudinal spar cap. The expansion-joint tie allows the transverse frame channels to move relative to each other as the skin panels expand or contract. The tie also provides continuity between skin panels so that their shear stiffness can be utilized for torsional stiffness of the model. For aerodynamic smoothness, the expansion joint is covered with a strip which is fastened on the upstream side.

In order to help isolate the longitudinal spar caps from the skin panels, the transverse frame channels cross the longitudinal spar cap on the outside. One channel in each frame is rigidly attached to the longitudinal cap but the other channel is freely floating so that the expansion-joint action is not restricted.

A skin sheet thickness of 0.010 inch was selected as minimum gage based on general concepts of noise failures and panel flutter. In order to better define design criteria for these phenomena, noise and flutter tests of this skin panel have been undertaken. Results to date of the noise tests indicate that cracking starts near the rivet line after 20 minutes exposure to 157 decibels of random frequency noise from an air jet. After 2 hours the cracks had lengthened but the panel had not broken up disastrously.

Flutter tests were run in the Langley Unitary Plan wind tunnel on 2-foot-square skin panels. Although the panel with the corrugations parallel to the air flow was more flutter resistant than one with the corrugations perpendicular to the air flow, both orientations withstood a dynamic pressure greater than 2,000 lb/sq ft.

TESTS AND DISCUSSION

In order to study the behavior of the structure when subjected to a simulated reentry environment, the laboratory test setup shown in figure 6 was constructed. The 12-foot-long model is cantilevered from a support at the left in figure 6. The model is mounted with the flat side up for convenience in testing. The testing simulates reentry conditions for a flat-bottom configuration. It should be pointed out that in the figures which follow, whenever top or bottom is mentioned, it refers specifically to the testing orientation of the model; thus the top skin refers to the flat side.

Raised above the model is a large radiator which heats the flat planform area. Planform temperature variations of 250° F are programed into seven control channels, and this variation of heat intensity can be seen in the radiator (fig. 6). Before a test, the radiator is lowered so that it is parallel to and about 4 inches above the flat surface of the model. Programed loading is applied hydraulically by jacks through the whipple-tree system into the underside of the model.

Figure 7 shows a typical programed test environment to which the structural model was exposed. Temperature and load are shown as a function of time up to 20 minutes. Since the model was a research specimen, no attempt was made to duplicate the effects of any specific reentry trajectory. Ramp function inputs were used to simplify the analysis of results. The temperature along the structural leading edge was increased at a rate of 10° F per second up to a maximum for the test series of $1,600^\circ$ F, then held constant for about 15 minutes, and finally decreased at a maximum programed rate of 10° F per second. These temperatures are comparable to structural temperatures which would be achieved in a lightly loaded unshielded vehicle or in a more heavily loaded vehicle behind a metallic heat shield. About midway in the test, a load pulse of 150 lb/sq ft was applied which produced maximum stresses of about 30 ksi in the structure.

Prior to the maximum cycle of heat and load at the level shown in figure 7, the model was subjected to about 100 cycles of loading up to 212 lb/sq ft at room temperature and 32 cycles of combined heating and loading at various levels of peak temperature between 400° F and $1,600^\circ$ F.

The measured distribution of temperature around the model cross section at a location 9 feet from the nose is given in figure 8. The general trend of the programed temperature variation of 250° F in the flat planform is evident in the top of the figure with the leading edges at about $1,600^\circ$ F and the center at $1,350^\circ$ F. The presence of

the two main spar caps lying beneath the heated skin shows up in the two intermediate peaks in the temperature curve. These spar caps are not conductive heat sinks because they are not in contact with the skin; but, since their proximity to the skin blocks the radiation, higher skin temperatures occur above the spars than on either side of the spars. A similar effect is not evident in the bottom skin inasmuch as the temperature levels are lower and radiation heat exchanges are much less. The temperatures shown in figure 8 are for 7 minutes of test time and correspond to approximately steady-state equilibrium for the skin panels.

Variation of temperature with time is shown in figure 9 for selected points on the top and bottom skins and top and bottom spar caps of the longitudinal beams. Temperature is plotted against time in minutes. The top skin shows a response very similar to the programed input (fig. 7) with the exception of the region near the end of the test when natural cooling took place at a slower rate than the maximum programed cooling rate. Heating of the spar caps and bottom skin occurred primarily by radiation from the top skin through the interior of the model. From 5 to 10 minutes elapsed after the top skin reached equilibrium before the other elements essentially reached equilibrium. The maximum temperature difference between the top and bottom spar caps occurs after approximately 7 minutes of test time.

Since the spar caps provide the longitudinal bending stiffness for the model, their temperature differences are reflected in the model deflection as shown in figure 10. Deflection of the model nose δ is plotted against time for the simulated reentry test. The total measured experimental deflection is given by the solid curve. It reaches a peak value of nearly 3 inches due to spar-cap temperature difference at about 7 minutes of test time corresponding to the maximum spar-cap temperature difference shown on the previous figure. Beyond this point, the deflection due to temperature difference decreases even though the absolute spar temperatures are still increasing.

The hump in the deflection curve is produced by the load pulse applied during the heating cycle. Note that deflection due to heating is about three times the deflection due to load. The rapid dropoff in deflection at $17\frac{1}{2}$ minutes corresponds to the time when peak heat input ceased and the entire model began to cool rapidly.

Computed deflections based on beam theory and using the measured temperatures inside the model are shown by the dashed curves in figure 10 for the conditions of heat and load which were superimposed during the test. The agreement between experimental and computed deflections is satisfactory considering the timewise and spacewise temperature variations.

A comparison of experimental and computed strains in the longitudinal compression spar cap is shown in figure 11 for a loading of 212 lb/sq ft on the planform area. Average load strain in the spar-cap cross section is shown as a function of distance from the rear. The solid curve is the computed value of average strain. The circles are average values of room-temperature strain measured with resistance strain gages located in several places on the cross section of the spar cap. The square is a measured load strain for the same applied load during a 1,000° F test. Agreement is shown between theory and experiment.

Figure 12 shows the condition of the structural model at the conclusion of the heating cycles. The only damage observed was a few local buckles in the hottest portions of the back two panels, that is, those with the largest planform temperature differences. Most of the buckles occurred in the two outlined regions and are small and confined to the beaded portion of the outer skin.

CONCLUDING REMARKS

A large structural model has been built incorporating design concepts applicable to a radiation-cooled vehicle. Some of the results of the test experience have been presented. The agreement shown between theory and experiment for deflections and strains indicates that beam bending theory is adequate to describe the average response of the model to applied loads and temperatures. On the basis of these results combined with visual inspection, it is concluded that these design concepts enabled the structure to survive successfully the simulated reentry heating and loading environments.

Langley Research Center,
    National Aeronautics and Space Administration,
        Langley Field, Va., April 12, 1960.

REFERENCES

1. Anderson, Roger A., and Swann, Robert T.: Structures for Reentry Heating. NASA TM X-313, 1960.

2. Pride, Richard A., Hall, John B., Jr., and Anderson, Melvin S.: Effects of Rapid Heating on Strength of Airframe Components. NACA TN 4051, 1957.

3. Peterson, James P., and Card, Michael F.: Investigation of the Buckling Strength of Corrugated Webs in Shear. NASA TN D-424, 1960.
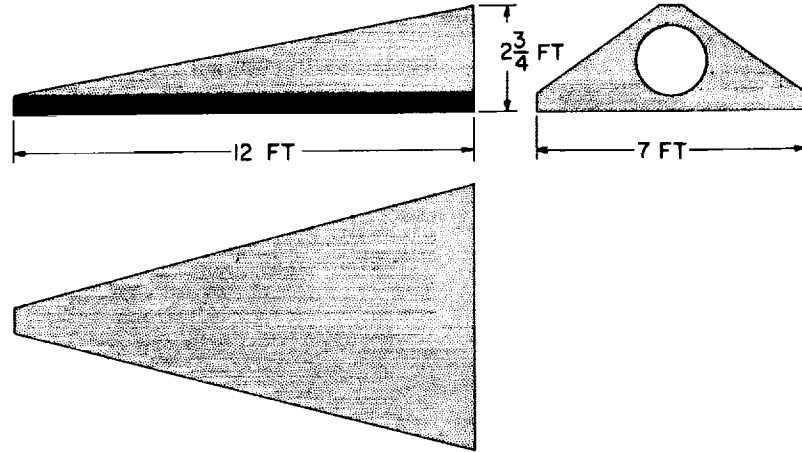
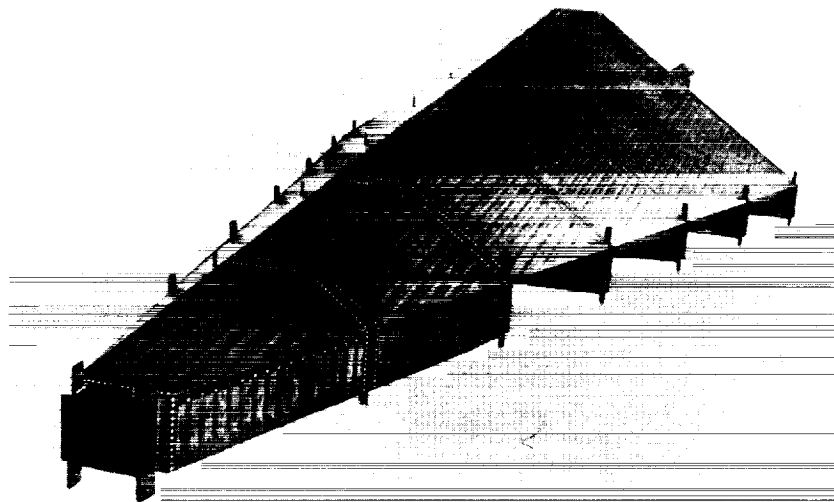STRUCTURAL – MODEL DIMENSIONS

Figure 1

STRUCTURAL-MODEL EXTERIOR

Figure 2   L-59-4915

STRUCTURAL-MODEL INTERIOR
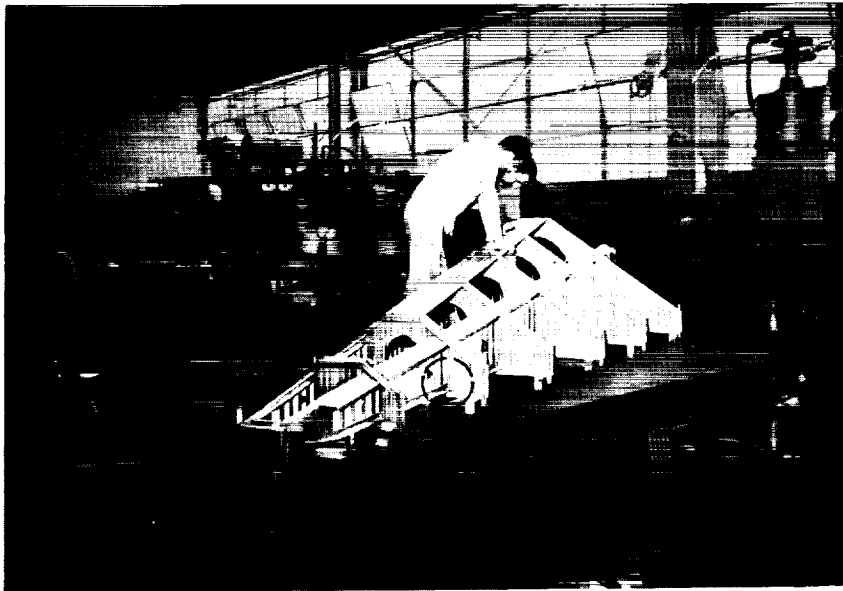
Figure 3   L-59-3377

INTERSECTION OF MODEL COMPONENTS
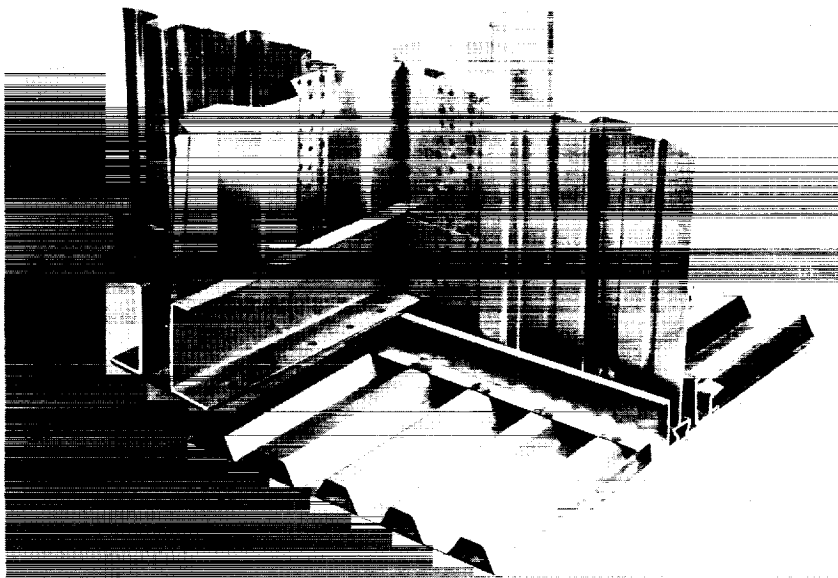
Figure 4   L-60-1152

EXPANSION-JOINT DETAIL

0   1   2   3
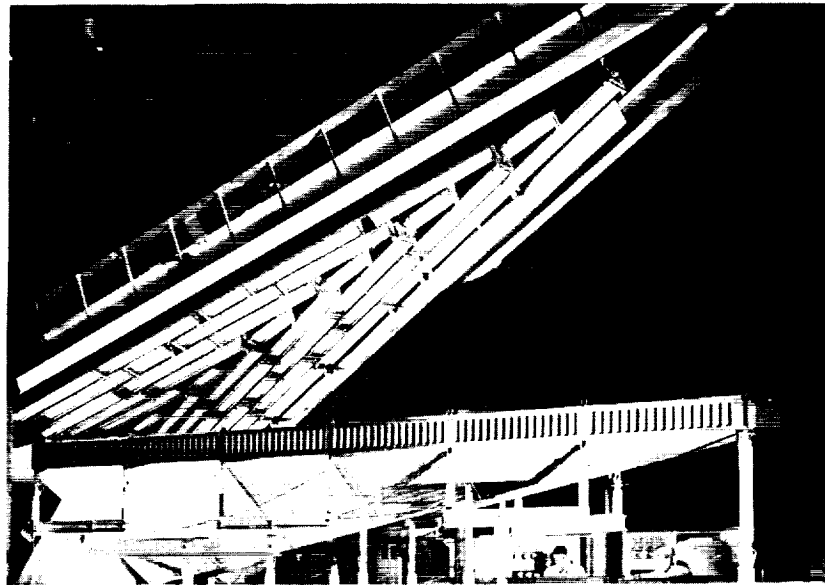
INCHES
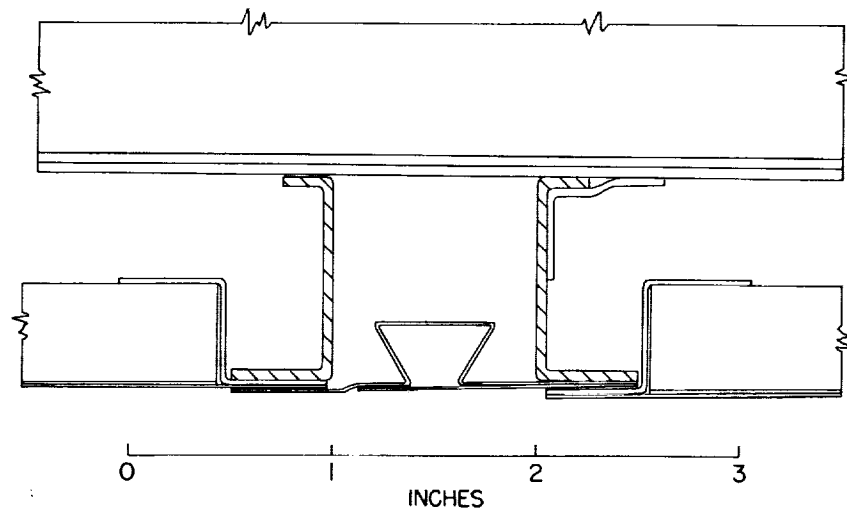
Figure 5

TEST SETUP

Figure 6   L-59-6745

PROGRAMED TEST ENVIRONMENT

Figure 7

TEMPERATURE VARIATION IN MODEL CROSS SECTION
STATION, 9 FEET FROM NOSE; TEST TIME, 7 MINUTES
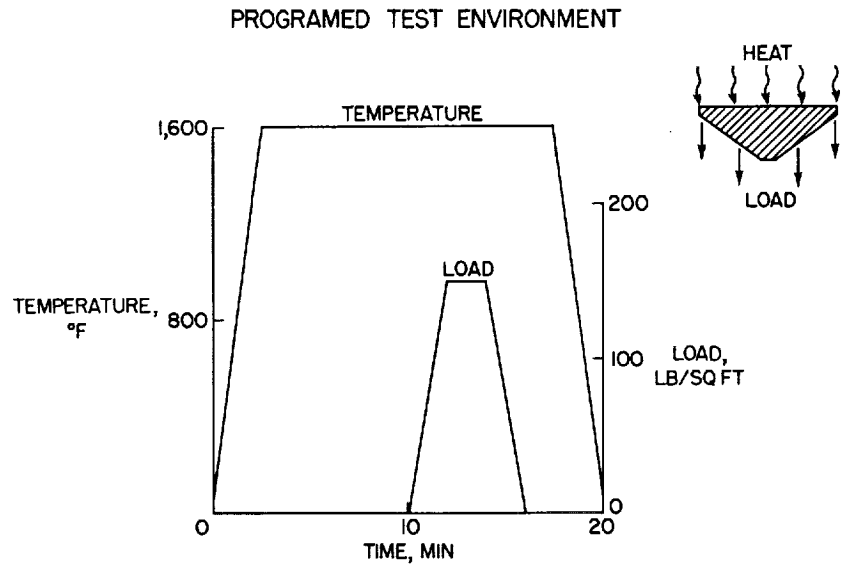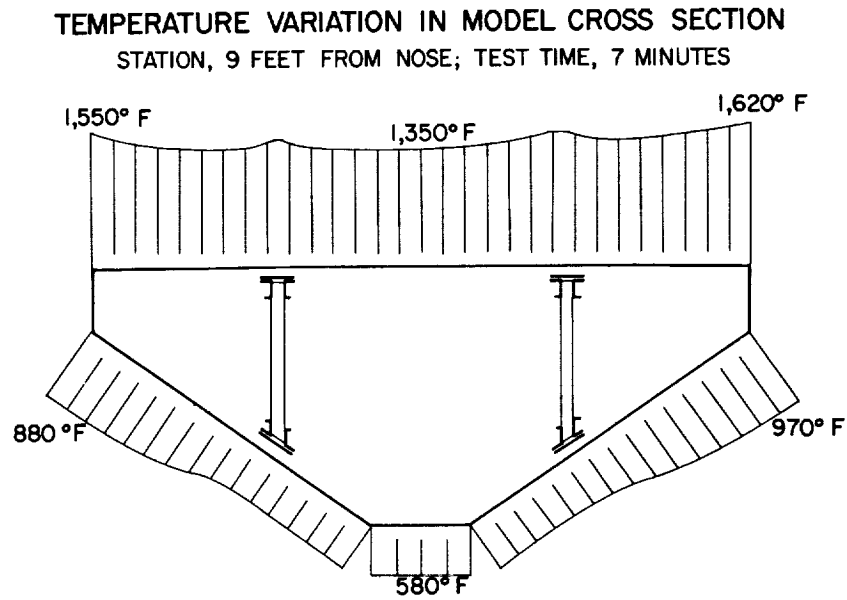
Figure 8

TIME – TEMPERATURE VARIATION IN MODEL CROSS SECTION
STATION, 9 FEET FROM NOSE

TEMP., °F

TOP SKIN

TOP SPAR

BOTTOM SPAR

BOTTOM SKIN

TIME, MIN
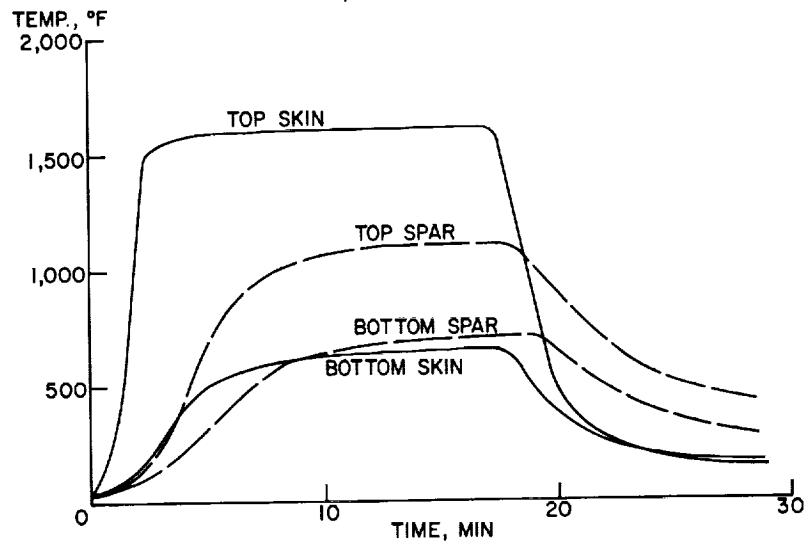
Figure 9

MODEL DEFLECTION DURING SIMULATED REENTRY

COMPUTED

EXPERIMENT

LOAD

HEAT

LOAD

δ, IN.

SPAR TEMPERATURE DIFFERENCE

TIME, MIN

Figure 10

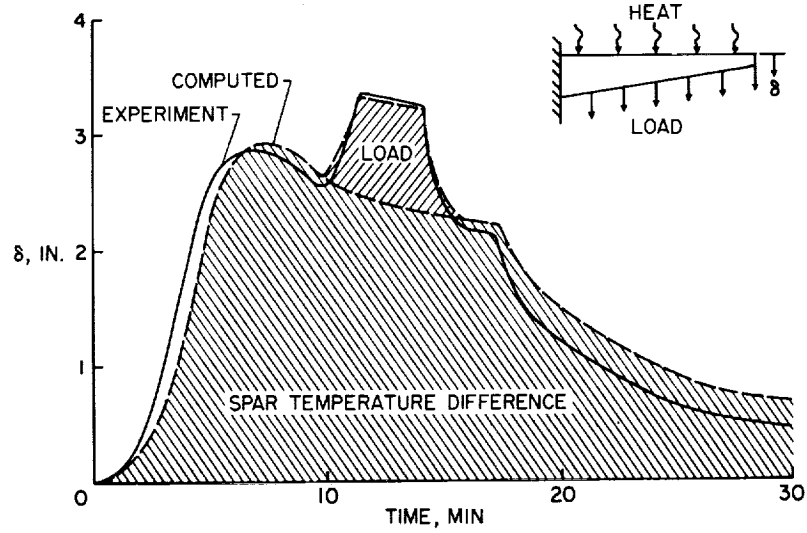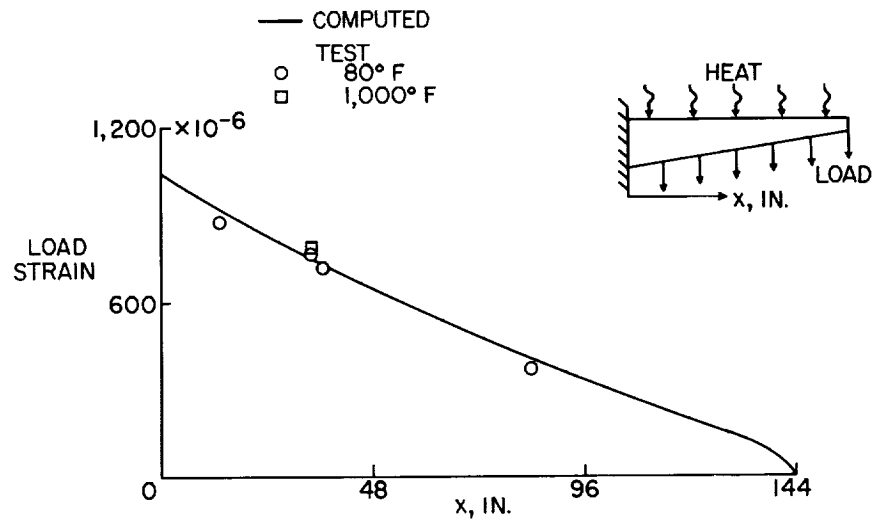## LOAD STRAIN IN COMPRESSION SPAR CAP
LOAD, 212 LB/SQ FT

Figure 11

CONDITION AFTER SIMULATED REENTRY

Figure 12   L-59-8645